

治療の安全性等に関して見解 (ICH considerations) やガイドラインの作成を行っている。ICH見解はガイドラインとは異なり各規制当局への拘束力はないものの、現時点での科学的な見解をICHとしてまとめたもので、参考にされることが望ましいものである。これまでにICH GTDGで取り上げられた主なトピックを表2に示した。これまでに3つの見解⁷を公表し、米国の長期フォローアップガイドラインやEMAのレンチウイルスベクターに関するガイドラインも議論された。これまでに発出された見解の概要を以下に紹介する。

1) 生殖細胞への遺伝子治療用ベクターの意図しない組み込みリスクに対応するための基本的な考え方

生殖細胞の意図的な遺伝子改変は日米欧すべてで禁止されているが、本見解はベクターの投与により、意図せずに生殖細胞に組み込まれるリスクをどのように試験し、どう対応すべきかの基本原則を明確にするとともに、ヒトでの臨床試験の実施に際して発生するリスクを最小にするための考慮事項を示したものである。非臨床試験で生体内分布試験により生殖組織にベクターが分布するか否かを調べることが求められており、非臨床試験で生殖細胞への分布が認められない場合でも、臨床試験期間中は避妊手段を取ることが推奨されている。

2) 腫瘍溶解性ウイルス

遺伝子治療の対象疾患はがんが6割以上を占めるが、従来のがん遺伝子治療薬では十分な有効性が得られにくく、様々な新しい治療薬の開発が試みられている。その一つが腫瘍溶解性ウイルスである。従来のがん遺伝子治療用ウイルスベクターは非増殖性ウイルスが用いられてきており、効果が感染細胞に限定されるが、腫瘍溶解性ウイルスはがん細胞で選択的に増幅して細胞を破壊するとともに、その際、放出されたウイルスが近隣のがん細胞や、遠隔転移細胞にも広がることで高いがん治療効果が期待されている。日米欧ではまだ承認品目はないが、中国では腫瘍溶解性アデノウイルス1品目が承認され、日本でもヘルペスウイルスやアデノウイルスを基にした腫瘍溶解性ウイルスの臨床開発が進められている。腫瘍溶

解性ウイルスは治療上の有用性が期待される一方で、複製能を有するウイルスを臨床で使用するというリスクとのバランスが重要であり、本見解はこのような腫瘍溶解性ウイルスの臨床開発のための一般原則を提示している。

3) ウイルスとベクターの排出に関する基本的な考え方

ウイルスやベクターの排出 (Shedding) とは、遺伝子治療薬の投与を受けた患者の分泌物や排泄物を介してウイルスやベクターが体外に拡散することを意味する。体外に排出されたウイルスやベクターは、医療従事者や家族などの第三者に伝播する公衆衛生上のリスクが懸念されるが、特にがん遺伝子治療分野で最近開発が進展している腫瘍溶解性ウイルスやがん免疫療法用のポックスウイルスベクター、腫瘍へのターゲティングやがん免疫促進アジュバントとして用いられる細菌ベクター等は増殖性があり、投与後に体内で増殖するため排出・伝播の懸念が高い。排出に伴う安全性上の問題は今までのところ確認されていないが、排出と伝播に関するデータの蓄積が求められている。本見解はウイルスやベクターの排出の可能性と伝播のリスクを評価するための基本的な考え方を提示したもので、非臨床及び臨床における排出試験のあり方、収集すべきサンプルの種類、サンプリングの頻度や期間、排出の分析法、結果の解釈等が提示されている。

5—今後の課題

我が国の遺伝子治療に関する2つの指針はいずれも国内初の遺伝子治療が開始される1995年頃に作成されたものが基となり、その後、数回の改正を経たものの、遺伝子治療の基本原則や品質・安全性確保の要件等の内容については15年以上経過した現在まで見直しが行われていない。この間、欧米やICHでは上述のとおり遺伝子治療の技術の進歩や経験の蓄積に対応して新たな指針・見解等を策定しており、我が国の指針も最新の科学の進歩や海外の規制動向を反映した見直しが必要と考えられる。また、日本の遺伝子治療は主に臨床研究として実施されているが、最近少し増加傾向が見られるものの欧米に比較して実施数はかなり少ない。これは遺

表2 ICH GTDGで取り上げられたトピック

● 生殖細胞へのベクターの組み込みリスク	} ICH見解の作成
● 腫瘍溶解性ウイルス (Oncolytic virus)	
● 患者からのウイルス/ベクターの排出 (Shedding)	
● ウイルス参照品 (Adenovirus type 5)	} -----> ガイドライン化検討
● 増殖性ウイルスの検出 (RCRやRCA)	
● X-SCID遺伝子治療における挿入変異によるがん化	} ICH見解作成検討
● 長期フォローアップ (FDA ガイドライン)	
● レンチウイルスベクター (EMA ガイドライン)	
● ファースト・イン・ヒューマン	
● 投与量の設定	

伝子治療臨床研究の申請手続きが煩雑で、審査に時間がかかることも一因と考えられている。そこで、厚生労働科学特別研究島田班⁸⁾において「遺伝子治療臨床研究に関する指針」の見直しが検討され、現行指針の問題点を抽出し、国内外の規制の動向等も考慮して新たな指針作成のための原案の検討が行われた。本原案は厚生労働科学研究成果データベースで公開予定であるが、主な改正点を表3に示した。原案では昨年改正された「ヒト幹細胞を用いる臨床研究に関する指針」や欧米の遺伝子治療関連指針を参考に、従来の指針ではほとんど記載のない被験者に投与する最終産物の品質・安全性評価に関しても指針別紙に詳しく記載した。また指針の対象を治療に限らず遺伝子導入を対象とすることでDNAワクチンも含め、臨床研究期間中の避妊や研究終了後の追跡調査の実施等について規制動向を取り込んだ。今後は、研究班が作成した原案を基に、厚生科学審議会での検討やパブリックコメントの聴取などを経て指針の改正が行われる予定である。本原案作成ではコンセンサスとして、臨床研究審査の効率化を目指すとしており、これまで以上に迅速な審査が行われることが期待される。

6—おわりに

欧米での遺伝子治療の規制動向や技術の進展を受けて、我が国でも指針の見直しが検討されている。改正案には従来の指針にはない新たな項目も追加されているが、これは規制強化を目的としたものではなく、我が国の遺伝子治療研究を活性化し迅速な臨床応用を可能にすることを目的としており、今後、指針改正に向けた公式の作業が早期に開始されることが望まれる。また、治療に適用される「遺伝子治療用医薬品の品質・安全性確保に関する指針」についても、最新の動向を反映した指針の改正や追加の指針策定等の作業が必要な時期が来ていると考えられ、厚生労働省の取り組みが待たれ

る。一方、ICH GTDGにより発出されるICH見解やガイドラインは、現行の国内指針ではカバーできていない点を埋める役割を果たしており、現在は活動が中断しているが、早期の活動再開が望まれる。これらの動きが遺伝子治療薬の適切かつ円滑な開発促進につながることを期待したい。なお、国内の遺伝治療の現状やICH GTDGの活動に関しては、国立医薬品食品衛生研究所遺伝子細胞医薬部ホームページ (<http://www.nihs.go.jp/cgtp/cgtp/home-j.html>) で公開しているので参考にいただければ幸いである。

参考文献

- 1) 遺伝子治療臨床研究に関する「遺伝子組換え生物等の使用等の規制による生物の多様性の確保に関する法律」に基づく第一種使用規程承認申請の手続等について（厚生労働省大臣官房厚生科学課長通知 科発第0219001号 平成16年2月19日）
- 2) Guidance for Industry: Guidance for Human Somatic Cell Therapy and Gene Therapy: Center for Biologics Evaluation and Research March 1998
- 3) Quality, Preclinical and Clinical Aspects of Gene Transfer Medicinal Products: CPMP BWP 3088 99 (Apr-01)
- 4) Guidance for Industry: Gene Therapy Clinical Trials - Observing Subjects for Delayed Adverse Events: Center for Biologics Evaluation and Research November 2006
- 5) FDA の遺伝子治療関連指針：
<http://www.fda.gov/BiologicsBloodVaccines/GuidanceComplianceRegulatoryInformation/Guidances/CellularandGeneTherapy/default.htm>
- 6) EMA の遺伝子治療関連指針：
http://www.ema.europa.eu/ema/index.jsp?curl=pages/regulation/general/general_content_000410.jsp&url=menus/regulations/regulations.jsp&mid=WC0b01ac058002958d
- 7) ICH considerations: <http://www.ich.org/products/consideration-documents.html>
- 8) 島田隆：遺伝子治療臨床研究推進のための指針見直しに向けた調査研究、厚生労働科学研究費補助金行政政策研究分野特別研究事業平成22年度総括研究報告書（厚生労働科学研究成果データベース文献番号201005014A）

表3 「遺伝子治療臨床研究に関する指針（案）」の主な改正点

- 全体構成：現行の章立てを見直し、単純で分かり易く再構成
臨床研究申請段階で必要とされる情報を具体的に記載
- 科学の進歩に合わせて遺伝子治療の定義及び適用範囲の再検討：指針の対象を明確化
- 多施設共同研究への対応
- 対象疾患の見直し：新規性のない遺伝子治療の規制を一部緩和
- 審査体制：施設内審査委員会と臨床研究作業委員会の役割の明確化、審査期間の短縮化
- 実施施設からの報告：報告の期限設定、研究経過報告の義務付け
- 情報の公開、記録の保存、インフォームド・アセントを含む人権保護に関する事項の記載

内田 恵理子 うちだ えりこ

国立医薬品食品衛生研究所
遺伝子細胞医薬部 第1室 室長
秋田県生まれ
東京大学 薬学部卒
東京大学大学院 薬学系研究科 修士課程修了
薬学博士
専門は遺伝子治療学、生物薬品化学

Kumiko Sakai-Kato¹
Shigenori Ota²
Kenji Hyodo³
Hiroshi Ishihara³
Hiroshi Kikuchi³
Toru Kawanishi¹

Short Communication

Size separation and size determination of liposomes

¹Division of Drugs, National Institute of Health Sciences, Setagaya-ku, Tokyo, Japan
²R&D Department, GL Sciences Inc., Iruma, Saitama, Japan
³DDS Research, Formulation Research Laboratories, Pharmaceutical Science and Technology Unit, Eisai Co. Ltd., Tsukuba-shi, Ibaraki, Japan

We developed a method for separating liposomes by size and determining their average diameters. Liposomes with different average diameters were separated on a monolithic silica capillary column, and the size of the liposomes corresponding to each peak was determined online with a dynamic light scattering detector coupled to the capillary liquid chromatography system. The calculated diameters for the separated liposomes were similar to the diameter values measured in batch mode. We demonstrate that this combination of a monolithic capillary column and light scattering detection could be used for size separation of liposomes and could provide more details about average diameters than batch-mode analysis.

Received May 13, 2011
Revised June 13, 2011
Accepted June 14, 2011

Keywords: Capillary liquid chromatography / Light scattering detection / Liposomes / Monolithic column
DOI 10.1002/jssc.201100417

1 Introduction

Advances in nanotechnology have contributed to the development of modern drug carrier systems, such as liposomes [1] and polymeric micelles [2, 3], that play an important role in the controlled delivery of pharmacological agents to their targets at a therapeutically optimal rate and dose [4]. Exact knowledge of the sizes of these nanoparticles is essential because size can substantially affect physico-chemical and biopharmaceutical behavior. For example, variations in particle size can affect drug release kinetics, transport across biological barriers, and pharmacokinetics in the human body [5–7].

Among the methods for the characterization of macromolecules, flow-assisted techniques, such as size-exclusion chromatography (SEC) [8, 9], hydrodynamic chromatography [10, 11], field-flow fractionation [12–14], and capillary hydrodynamic fractionation [15], are suitable for separation on the basis of differences in the physical size indexes of the analytes. Electrophoretic separation methods are also used for separation and characterization of colloids that are charged in buffered aqueous solutions [16–18].

SEC is the most commonly used fractionation method for particle sizing. Usually, SEC is performed on a column packed with polymer gel or porous silica microparticles with various pore-size distributions. Polymer samples are separated with such packed SEC columns [8], and nanoparticu-

late drug carriers, such as liposomes, are often separated from small solutes by means of SEC [19].

Recently, macromolecules, such as a polystyrene polymer, were separated on monolithic silica columns by SEC [20]. Monolithic columns have received much attention as a new technology for HPLC and capillary electrochromatography [21, 22]. These columns consist of a single piece of porous material (most often polymer- or silica-based) with a bimodal pore structure consisting of through-pores (pore size ~1.5–5 μm) and mesopores in the skeleton (~10–25 nm) [23]. Because of the high porosity of the monolithic columns, they can be lengthened, thus leading to high separation efficiency.

Although the elution profile obtained by means of SEC provides insight into size distribution, it does not give information about absolute particle size. Dynamic light scattering (DLS), also known as photon correlation spectroscopy, is a non-invasive technique for measuring the size of molecules and particles, typically in the submicron region; and with the latest technology, particles sizes of <1 nm have been measured. DLS is routinely used for size and polydispersity measurements, along with aggregate quantification.

In this report, we describe a system that combines the high resolution of capillary LC with acquisition of absolute diameter data by means of DLS for the online size separation and size determination of liposomal formulations. Although a system using conventional LC coupled with DLS has already been reported [24], ours is the first system that uses capillary LC coupled with DLS.

2 Materials and methods

2.1 Liposome preparation

Liposome samples were prepared by an extrusion procedure. A lipid film containing dipalmitoylphosphatidylcholine,

Correspondence: Dr. Kumiko Sakai-Kato, Division of Drugs, National Institute of Health Sciences, 1-18-1 Kamiyoga, Setagaya-ku, Tokyo 158-8501, Japan
E-mail: kumikato@nihs.go.jp
Fax: +81-3-3700-9662

Abbreviations: DLS, dynamic light scattering; SEC, size-exclusion chromatography

cholesterol, and dipalmitoylphosphatidylglycerol (30:40:30, lipid content 20 mM) was suspended in 9.5% sucrose. The suspension was extruded through 200-, 100-, 80-, and 50-nm polycarbonate membranes in that order. Extrusions at every pore size were repeated. Extruded liposome samples were stored in the refrigerator. Samples were dissolved or dispersed in eluent and filtered through a 0.20- μ m filter (Millex-LG, Millipore, Tokyo, Japan) prior to being applied to the columns. We used two liposomes with average diameters of 77 and 155 nm, as measured by batch-mode analysis in 10 mM sodium phosphate buffer (pH 7.2) containing methanol (5% v/v), which was also the solvent used as the chromatography eluent.

2.2 LC conditions

The schematics of the analytical system we developed are shown in Fig. 1. Separation was performed with a capillary LC system equipped with a capillary LC micro-flow pump (MP711V; GL Sciences, Tokyo, Japan), a four-port internal sample injector (fixed volume 10 nL; Valco Instrument, Houston, TX, USA), and a capillary ultraviolet-visible (UV-vis) detector (MU701; GL Sciences). Samples were analyzed on a MonoCap Amide column (500 mm \times 0.2 mm id; mesopore size \sim 15 nm or \sim 20 nm; GL Sciences). The total porosity of the column was estimated using void times of hollow capillary column and monolithic capillary column, and total volume of the column. The eluent was 10 mM sodium phosphate buffer (pH 7.2) containing methanol (5% v/v). The eluent was delivered at a flow rate of 0.1 μ L/min, and the column was kept at room temperature. The capillary UV-vis detector was operated at a wavelength of 210 nm. A sample volume of 10 nL was injected for each analysis. Downstream of the UV-vis detector, the same eluent was added by means of a semi-micro-flow pump (NanoSpace 3101 SI-2, Shiseido, Tokyo, Japan) through a T-joint to increase the flow rate. At the increased flow rate, the eluate

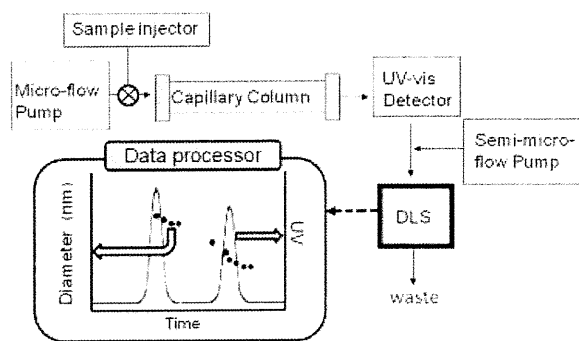


Figure 1. Schematic of analytical system for size separation of liposomes and determination of their average diameters. Samples were injected onto a monolithic capillary column and detected by a microLC UV-vis detector. The flow rate was increased downstream of the detector by means of a semi-micro-flow pump. At the increased rate, the eluate from the UV detector flowed continuously into the DLS detector.

from the UV-vis detector continuously flowed into the flow cell of a DLS detector via a reducing joint (2 mm, 1/16 inch, GL Sciences). Zetasizer Software was used to calculate the average diameters of the liposomes. A real-time parameter reading from the external device (the UV-vis detector in this case) can be also directly introduced into the optics unit and added to the light scattering sample record.

3 Results and discussion

3.1 Separation of liposomes on the monolithic capillary column

In this report, we used the monolithic column which consisted of silica derivatized with an amide group, a neutral hydrophilic group that prohibits adsorption of the samples on the silica monolith by ion-exchange interactions and that permits the analysis of charged soft nanocarriers, such as liposomes derived from biomaterials. As the eluent, 10 mM sodium phosphate buffer (pH 7.2) containing methanol (5% v/v) was used. We attempted to separate liposomes with two different average diameters on a monolithic column with mesopore size of \sim 15 nm. However, this column did not effectively separate the liposomes (Fig. 2A). When we used a monolithic column with larger mesopores (average size \sim 20 nm), the resolution was improved (Fig. 2B). Because total porosity is also

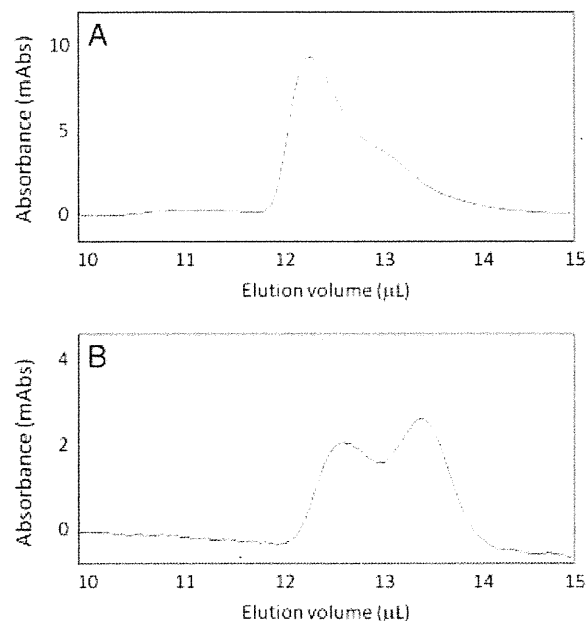


Figure 2. Effect of mesopore size on the separation of liposomes on monolithic columns with (A) \sim 15-nm mesopores and (B) \sim 20-nm mesopores. Column: capillary EX nano MonoCap Amide (500 mm \times 0.2 mm id); eluent: 10 mM phosphate buffer (pH 7.2) containing 5% methanol; sample: mixture of liposomes with diameters of 155 and 77 nm, as determined by batch measurement; flow rate: 0.1 μ L/min; detection wavelength: 210 nm.

increased from 88 to 95%, it is presumed that an increase in throughpore volumes also contributed to the improvement of resolution. SEM images of the latter monolithic column showed the presence of rough surfaces (micron and submicron ranges; Fig. 3). Typically, monolithic columns are more porous than conventional columns packed with spherical particles, and the higher porosity results in much lower column backpressure. Furthermore, the throughpore/skeleton size ratio of 2–4 for the monolithic column was much greater than the 0.25–0.4 ratio typical of columns packed with particles [25]. This higher ratio permits the use of a long column and thus high separation efficiency [26]. Therefore, we connected three 500-mm columns (total length 1500 mm) and then tried the separation again. As expected, the resolution was further improved (Fig. 4A), and the column pressure was only 1.5 MPa. In contrast, the same two liposomes could not be separated by batch-mode DLS analysis (Fig. 4B), and these results show the usefulness of the monolithic column. Also, there is no report that SEC using conventional LC can obtain such a high resolution of liposomes with two different average diameters within 100-nm range. We could not separate liposomes with two different average sizes (111 and 77 nm)

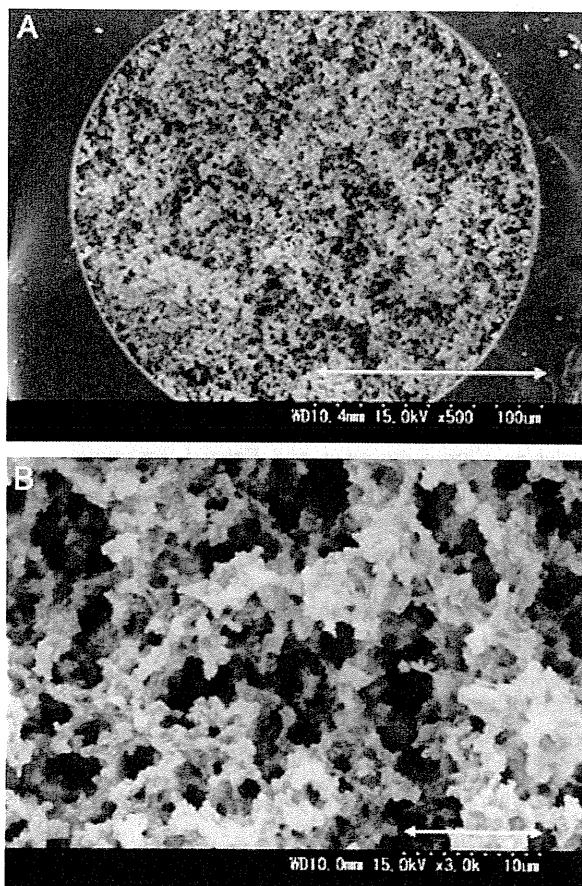


Figure 3. Scanning electron micrographs of monolithic capillary columns. Scale bars correspond to 100 μm for (A) and 10 μm for (B).

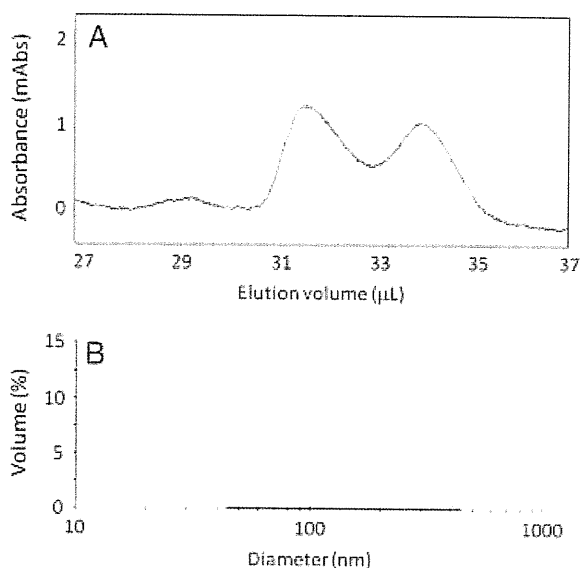


Figure 4. Analysis of liposomes in (A) flow-assisted mode and (B) batch mode. (A) Analysis in flow-assisted mode. Column: capillary EX nano MonoCap Amide (500 mm \times 0.2 mm id) \times 3; eluent: 10 mM phosphate buffer (pH 7.2) containing 5% methanol; sample: mixture of liposomes with sizes of 155 and 77 nm, as determined by batch measurement; flow rate: 0.1 $\mu\text{L}/\text{min}$; detection wavelength: 210 nm. (B) Analysis in batch mode with DLS detection. Sample: mixture of liposomes with diameters of 161 and 77 nm; dispersant: 10 mM phosphate buffer (pH 7.2) containing 5% methanol.

(data not shown). Therefore, the separation of 80 nm size difference is possible by this system.

3.2 Online data acquisition by DLS

Next, we evaluated a system that combined capillary LC with DLS detection. The DLS data were accumulated continuously and analyzed every 3 s, and the software recorded all correlation functions and intensity values. Because the volume of the DLS flow cell was 135 μL and the detection volume was 5 μL , and the flow rate of the capillary LC system was $<1 \mu\text{L}/\text{min}$, we increased the flow rate downstream of the UV–vis detector by adding the same eluent to the flow by means of a semi-micro-flow pump through a T-joint downstream of the detector. However, the flow was diluted by the additional eluent. Therefore, we examined the effect of the increased flow rate on the intensity of scattered light to make sure that DLS detection was still feasible at the higher flow rate. At flow rates ranging from 50 to 10 $\mu\text{L}/\text{min}$, DLS detection was possible, and diameters of the liposomes could be calculated. Figure 5A shows the average diameter and external UV input for monodisperse liposomes injected onto the monolithic column. The system was operated at a flow rate of 50 $\mu\text{L}/\text{min}$. From the single peak that was detected, we calculated an average diameter of 166 nm, which was close to the expected value (155 nm) for this liposome dispersion, as indicated by batch-mode

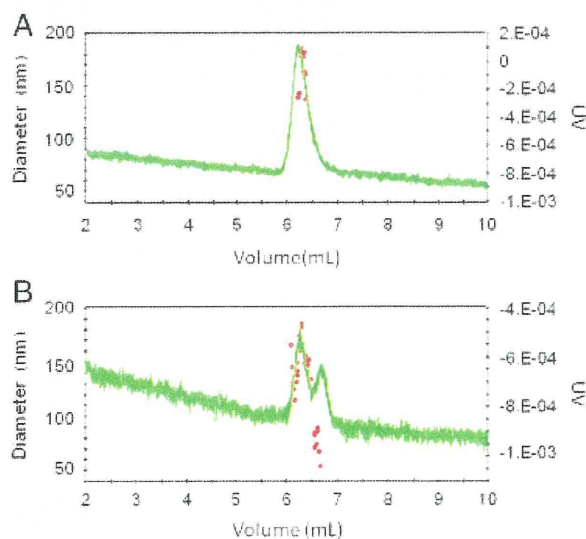


Figure 5. Plots of diameters and UV absorption versus elution volumes for liposomes injected onto a monolithic column. Column: capillary EX nano MonoCap Amide (500 mm × 0.2 mm id); eluent: 10 mM phosphate buffer (pH 7.2) containing 5% methanol; sample: liposomes with diameters of (A) 155 nm and (B) mixture of liposomes with diameters of 155 and 77 nm as determined by batch measurement. Capillary LC flow rate: 0.1 μ L/min; semi-micro-flow pump flow rate: 50 μ L/min; detection wavelength: 210 nm. AU: arbitrary unit.

analysis. We ascribed the similarity of the values to the low column backpressure, which did not affect the diameter of liposomes. The run-to-run repeatability of the calculated diameter for the eluted sample was determined to be 1.2% (RSD, $N = 3$). As far as I know, there have been no reports that the semi-micro-LC column or conventional column can separate liposomes with two different average diameters within 100-nm range. If we can use semi-micromonolithic LC column or conventional monolithic column long enough to separate liposomes with two different average diameters within 100-nm range, it is not required to dilute eluate from column before detector.

Next, we used the developed system to analyze a dispersion of liposomes with two different diameter ranges. Figure 5B shows the diameter and external UV input versus elution volumes for liposomes, separated onto a monolithic column. The size separation of the liposomes was good, and average diameters for the two detected peaks were calculated as 164 and 77 nm; these values were also similar to the values measured in batch mode, 155 and 77 nm, respectively.

4 Concluding remarks

We developed a system for simultaneous size separation and size determination of liposomes using a capillary LC system with DLS detection. By changing the mesopore size, we could improve the separation of liposomes with different

average diameters. Because the column had a low backpressure, resolution could easily be increased by lengthening the column. After increasing the flow rate with a second pump, we used DLS detection to determine the diameters of the separated liposomes. Analysis with this system provided more-detailed information than conventional batch-mode analysis about the size of the liposomes, which affects their physicochemical and biopharmaceutical behavior.

The authors are grateful for financial support from the Research on Publicly Essential Drugs and Medical Devices Project (The Japan Health Sciences Foundation), a Health Labor Sciences Research Grant from the Ministry of Health, Labor and Welfare (MHLW), and KAKENHI (21790046) from the Ministry of Education, Culture, Sports, Science, and Technology (MEXT), Japan.

The authors have declared no conflict of interest.

5 References

- [1] Bangham, A. D., Standish, M. M., Watkins, J. C., *J. Mol. Biol.* 1965, **13**, 238–252.
- [2] Nishiyama, N., Kataoka, K., *Pharmacol. Ther.* 2006, **112**, 630–648.
- [3] Torchilin, V. P., Lukyanov, A. N., Gao, Z., Papahadjopoulos-Sternberg, B., *Proc. Natl. Acad. Sci. USA* 2003, **100**, 6039–6044.
- [4] Ferrari, M., *Nat. Rev. Cancer* 2005, **5**, 161–171.
- [5] Hillyer, J. F., Albrecht, R. M., *J. Pharm. Sci.* 2001, **90**, 1927–1936.
- [6] Lamprecht, A., Bouligand, Y., Benoit, J. P., *J. Control Release* 2002, **84**, 59–68.
- [7] Rejman, J., Oberle, V., Zuhorn, I. S., Hoekstra, D., *Biochem. J.* 2004, **377**, 159–169.
- [8] Kirkland, J. J., *J. Chromatogr. A* 1976, **125**, 231–250.
- [9] Huang, S. S., in: Wu, C.-S. (Eds.), *Handbook of Size Exclusion Chromatography and Related Techniques*, Marcel Dekker, New York 2004, p. 677.
- [10] Small, H., Colloid, J., *Interface Sci.* 1974, **48**, 147–161.
- [11] Williams, A., Varela, E., Meehan, E., Tribe, K., *Int. J. Pharm.* 2002, **242**, 295–299.
- [12] Giddings, J. C., *Science* 1931, **260**, 1456–1465.
- [13] Giddings, J. C., *Anal. Chem.* 1995, **67**, 592A–598A.
- [14] Moon, M. H., Park, I., Kim, Y., *J. Chromatogr. A* 1998, **813**, 91–100.
- [15] Silebi, C. A., Dosramos, J. G., *J. Colloid. Interface Sci.* 1989, **130**, 14–24.
- [16] VanOrman, B. B., McIntire, G. L., *J. Microcolumn Sep.* 1989, **1**, 289–293.
- [17] Ahmadzadeh, H., Dua, R., Presley, A. D., Arriaga, E. A., *J. Chromatogr. A* 2005, **1064**, 107–114.
- [18] Rezenom, Y. H., Wellman, A. D., Tilstra, L., Medley, C. D., Gilman, S. D., *Analyst* 2007, **132**, 1215–1222.

- [19] Grabielle-Madellmont, C., Lesieur, S., Ollivon, M., *J. Biochem. Biophys. Methods* 2003, *56*, 189–217.
- [20] Ute, K., Yoshida, S., Kitayama, T., Bamba, T., Harada, K., Fukusaki, E., Kobayashi, A., Ishizuka, N., Minakuchi, H., Nakanishi, K., *Polymer J.* 2006, *38*, 1194–1197.
- [21] Minakuchi, H., Nakanishi, K., Soga, N., Ishizuka, N., Tanaka, N., *Anal. Chem.* 1996, *68*, 3498–3501.
- [22] Peters, E. C., Petro, M., Svec, F., Frechet, J. M. J., *Anal. Chem.* 1998, *70*, 2296–2302.
- [23] Tanaka, N., Kobayashi, H., Nakanishi, K., Minakuchi, H., Ishizuka, N., *Anal. Chem.* 2001, *73*, 420A–429A.
- [24] Zetasizer nano application note, Absolute size exclusion chromatography, MRK877-01, Malvern. [http://www.malvern.com/malvern/kbase.nsf/allbyno/KB001244/\\$file/MRK877-01.pdf](http://www.malvern.com/malvern/kbase.nsf/allbyno/KB001244/$file/MRK877-01.pdf).
- [25] Unger, K. K., *Porous Silica (Journal of Chromatography Library–vol. 16)*, Elsevier, Amsterdam 1979.
- [26] Miyamoto, K., Hara, T., Kobayashi, H., Morisaka, H., Tokuda, D., Horie, K., Koduki, K., Makino, S., Núñez, O., Yang, C., Kawabe, T., Ikegami, T., Takubo, H., Ishihama, Y., Tanaka, N., *Anal. Chem.* 2008, *80*, 8741–8750.

Stabilization of Liposomes in Frozen Solutions Through Control of Osmotic Flow and Internal Solution Freezing by Trehalose

KEN-ICHI IZUTSU, CHIKAKO YOMOTA, TORU KAWANISHI

National Institute of Health Sciences, Setagaya-ku, Tokyo 158-8501, Japan

Received 22 September 2010; revised 7 December 2010; accepted 25 January 2011

Published online 16 February 2011 in Wiley Online Library (wileyonlinelibrary.com). DOI 10.1002/jps.22518

ABSTRACT: The purpose of this study was to elucidate the effect of trehalose distribution across the membrane on the freeze-related physical changes of liposome suspensions and their functional stability upon freeze–thawing. Cooling thermal analysis of 1,2-dipalmitoyl-*sn*-glycero-3-phosphocholine liposome suspensions showed exotherm peaks of bulk (–15°C to –25°C) and intraliposomal (approx. –45°C) solution freezing initiated by heterogeneous and homogeneous ice nucleation, respectively. The extent of the intraliposomal solution freezing exotherm depended on liposome size, lipid composition, cosolutes, and thermal history, suggesting that osmotic dehydration occurred due to the increasing difference in solute concentrations across the membrane. A freeze–thawing study of carboxyfluorescein-encapsulated liposomes suggested that controlling the osmotic properties to avoid the freeze-induced intraliposomal solution loss either by rapid cooling of suspensions containing trehalose in both sides of the membrane (retention of the intraliposomal supercooled solution) or by cooling of suspensions containing trehalose in the extraliposomal media prior to freezing (e.g., osmotic shrinkage) led to higher retention of the water-soluble marker. Evaluation and control of the osmotically mediated freezing behavior by optimizing the formulation and process factors should be relevant to the cryopreservation and freeze-drying of liposomes. © 2011 Wiley-Liss, Inc. and the American Pharmacists Association *J Pharm Sci* 100:2935–2944, 2011

Keywords: liposomes; formulation; stabilization; thermal analysis; osmosis; calorimetry (DSC); excipients; freeze-drying

INTRODUCTION

The increase in the variety and clinical relevance of liposomal formulations has enhanced the importance of the freezing and freeze-drying processes for the distribution and long-term storage of the drug delivery systems that are not chemically and/or physically stable enough as aqueous suspensions.^{1–4} These processes, however, expose the lipid systems to various stresses including ice growth, pH change, concentration of the surrounding solutes, and dehydration that often damage their structural integrity and pharmaceutical functions [e.g., release of active pharmaceutical ingredients (APIs)] of liposomes. Retaining water-soluble APIs is a particular challenge for development of liposome formulations.¹ Formulation and process design that are based on an understand-

ing of the freeze-related stresses and required stabilization mechanisms should improve the stability of various liposome pharmaceuticals.^{1–3}

Disaccharides (e.g., trehalose and sucrose) and some amino acids have been applied to protect the lipid systems from chemical and physical changes during freeze–thawing (cryoprotectants) and freeze-drying (lyoprotectants).^{1,3} The stabilization of liposomes by disaccharides is explained mainly by three mechanisms. Some saccharides substitute the water molecules necessary to retain the supramolecular phospholipid assembly through molecular interactions with hydrophilic phospholipid head groups (water substitution).^{5–7} The saccharides also form highly viscous amorphous freeze-concentrated phases and dried solids that prevent direct contact between liposome vesicles (bulking).^{1,8,9} The reduced mobility of the surrounding molecules helps improve the chemical and physical stability of liposomes (vitrification). Use of the stabilizers is mostly dependent on empirical trial and error through analysis of the morphological (e.g., size) and functional (e.g., API or marker

Correspondence to: Ken-ichi Izutsu (Telephone: +81-3-3700-1141; Fax: 81-3-3707-6950; E-mail: izutsu@nih.go.jp)

Journal of Pharmaceutical Sciences, Vol. 100, 2935–2944 (2011)

© 2011 Wiley-Liss, Inc. and the American Pharmacists Association

retention) traits of the resulting suspensions or dried solids.

Longstanding cryopreservation studies of living cells and microorganisms provide precepts valuable for the protection of liposomes against the freeze-induced stresses.^{10–14} The cooling of cell and liposome suspensions induces the freezing of bulk solutions initiated by heterogeneous ice nucleation at the surface of containers or impurities (-5°C to -25°C) and the freezing of spatially restricted internal solutions initiated by homogeneous (spontaneous) ice nucleation (-25°C to -45°C).^{15–21} The bulk solution freezing and the accompanying significant concentration of solutes surrounding the living cells and liposomes induce osmotic stress that removes the internal solution before they freeze, leading to morphological changes observable by microscopic methods (e.g., optical microscope and cryo-transmission electron microscopy).^{21,22} Because the intracellular ice formation (IIF) is widely recognized to cause lethal damage through disordering of the complex membrane and intracellular structure (e.g., organelle), cryopreservation of the living cells and microorganisms is usually performed in two ways that prevent IIF, namely by slow cooling of suspensions containing extracellular solutes (cell dehydration) and by rapid cooling of the suspensions containing high-concentration membrane-permeating solutes [e.g., dimethyl sulfoxide (DMSO), cytoplasm vitrification].¹² On the contrary, only limited studies have been performed on the stabilization of liposomes taking various freezing-related physical changes into account.^{17,23–25}

The purpose of this study was to elucidate the effect of intra- and extraliposomal trehalose on the freeze-related physical changes and functional stability of liposomes during freeze-thawing. The effect of saccharide distribution across the membrane on the stability of liposomes is of particular interest for formulation purposes because the liposome preparation methods significantly affect allocation of the nonpermeating solutes. Different solute concentrations across the membrane induce osmotic flow that shrinks or swells the liposomes in the aqueous suspensions.^{4,22,26} Literature claims the requirement of disaccharides on both sides of the membrane to protect liposomes from freezing- and lyophilization-related stresses (e.g., addition before extrusion).⁸ Recent reports suggested that the rational setting of different intra- and extraliposomal trehalose concentrations confers better stabilization.^{1,27} Effect of trehalose on the freeze-related physical phenomena (e.g., freeze-induced dehydration and intraliposomal solution freezing) and functional stability of liposomes were studied mainly through thermal analysis and through the retention of encapsulated carboxyfluorescein (CF).^{27,17}

MATERIALS AND METHODS

Materials

Chemicals obtained from the following sources were used without further purification: 1-palmitoyl-2-oleoyl-*sn*-glycero-3-phosphocholine (POPC), 1,2-dimyristoyl-*sn*-glycero-3-phosphocholine (DMPC), 1,2-dipalmitoyl-*sn*-glycero-3-phosphocholine (DPPC), and 1,2-distearoyl-*sn*-glycero-3-phosphocholine (DSPC) (NOF Co., Tokyo, Japan); trehalose dihydrate, glucose, sucrose, and 5(6)-CF (Sigma-Aldrich Co., St. Louis, Missouri); DMSO, xylitol, and glycerol (Wako Pure Chemical Co., Osaka, Japan); and dextran 4000–6000 (Serva Electrophoresis GmbH, Heidelberg, Germany).

Preparation of Liposome Suspensions

Phospholipid films were obtained by drying their solution in a chloroform and methanol mixture (2:1) under vacuum at temperatures above the main transition temperature (T_m). Liposome suspensions were prepared by using a hand-held extruder (Avanti Polar Lipids, Alabaster, Alabama). The films hydrated by 10 mM Tris-HCl buffer (6%, w/w; pH 7.4) were extruded 12 times through a polycarbonate membrane filter (0.1–0.8 μm pore, 0.2 μm unless otherwise mentioned; Whatman, Maidstone, UK) while maintaining the apparatus at room temperature (POPC) or at temperatures 10 to 15 $^{\circ}\text{C}$ higher than the T_m of the respective lipids. The DPPC liposomes extruded through the smaller pore membranes (0.1 and 0.2 μm) were reported to have a unilamellar structure, whereas those extruded through the larger pore membranes (0.4 and 0.8 μm) contained increasing ratios of multilamellar vesicles.^{29,30} The term “0.2 μm liposome” will be used in the text given below to denote samples prepared by extrusion through the respective pore size membranes.

Some liposome suspensions containing the excipients predominantly in the extraliposomal media were prepared by adding the excipients approximately 30 min prior to the thermal analysis and freeze-thawing experiments. Those containing excipients in both the inside and outside of the membranes were prepared by the extrusion of lipids hydrated with the excipient-containing solutions. Some suspensions were eluted through Sephadex G-25 desalting columns (PD-10; GE Healthcare Bio-Sciences AB, Uppsala, Sweden) equilibrated with the Tris-HCl buffer to obtain samples containing the excipient mainly in the intraliposomal solutions. The concentrations of DPPC in the column-eluted suspensions were obtained by phosphorous assay.³¹ Measurement of the DPPC concentrations in the liposome suspensions indicated that approximately 90% of the liposomes passed through the Sephadex columns.

Thermal Analysis

Thermal analysis of the frozen liposome suspensions was performed by using a differential scanning calorimeter (DSC Q10; TA Instruments, New Castle, Delaware) equipped with a refrigerating system and data processing software (Universal Analysis 2000, TA Instruments). Aliquots [10 μ L, 4% (w/w) lipid] of suspensions in hermetic aluminum cells were cooled from 25°C to -70°C at varied speeds (1–10°C/min) and then heated to 25°C at a scanning rate of 5°C/min. The intensity of the intraliposomal solution freezing exotherm was shown as their ratio to the lipid content (J/g lipid). Some DPPC liposome suspensions were heat-treated at 45°C for 3 min before the cooling scan. The cooling scan of some suspensions were paused at certain temperatures (-10°C to -35°C) and maintained those temperatures for 30 or 60 min before further cooling to study the effect of low temperature storage on the physical changes. The column-eluted liposome suspensions were subjected to thermal analysis without the concentration adjustment. The homogeneous ice formation exotherms of these suspensions were calculated using the phosphate concentration data.

Measurement of Liposome Size by Dynamic Light Scattering

The size distribution of liposomes suspended in the Tris-HCl buffer (0.08% DPPC, 25°C) was determined using a dynamic light scattering (DLS) spectrophotometer (Photal DLS-7100SL; Otsuka Electronics Co., Osaka, Japan) with a He-Ne laser (632.8 nm) and a scattering angle (90°; 50 scans).

CF Retention Study

Dried DPPC films were hydrated with solutions containing 25 mM 5(6)-CF, 10 mM Tris-HCl buffer, and 0% or 12% trehalose, adjusted to pH 7.4 by NaOH. The CF-loaded vortexed multilamellar liposome suspensions (6% lipid, w/w) were prepared by extrusion through a 0.2- μ m pore filter, and then eluted through the Sephadex G-25 column equilibrated with the buffer or trehalose-containing buffer. Freeze-thawing of the suspension was performed using the DSC system while the thermal profiles were simultaneously monitored. Aliquots of the liposome suspensions (10 μ L, 4% DPPC, w/w) in unsealed aluminum pans were cooled to -35°C or -70°C at varied cooling speeds (1–10°C/min), and then heated to 25°C at 10°C/min on the DSC furnace. The freeze-thawed liposome suspensions were diluted by adding the Tris-HCl buffer or trehalose-containing buffer solutions (10 mL) in the glass tubes. The mildly agitated liposome suspensions underwent fluorescence measurement using a spectrometer (FP-6500; JASCO

Corp., Tokyo, Japan). After the initial fluorescence measurements of the suspensions (2 mL) at 460 nm (excitation) and 550 nm (emission), those of the membrane-perturbed liposome suspensions were obtained by the addition of aliquots (20 μ L) of Triton X-100. The CF leakage ratio was calculated using the following equation:

$$\begin{aligned} \% \text{ Leakage} = & \\ & \frac{\text{Initial fluorescence of treated sample} \\ & - \text{initial fluorescence of control}}{\text{(Final fluorescence of treated sample} \\ & - \text{initial fluorescence of control)}} \\ & \times 100 \end{aligned}$$

RESULTS AND DISCUSSION

Freeze-Induced Changes in Liposome Suspensions

Figure 1 shows a thermogram of a frozen DPPC liposome suspension (4% in 10 mM Tris-HCl buffer, 0.2 μ m) cooled at 5°C/min. The suspension showed a large exothermic peak of the freezing of the bulk solution (heterogeneous ice nucleation) at approximately -20°C and a smaller second exothermic peak of the freezing of the intraliposomal solution (homogeneous ice nucleation) at approximately -45°C.^{15,17,32} The lower temperature exotherm disappeared by prior addition of a membrane-perturbing surfactant (1% Triton X-100), which supported the aforementioned definition of the peak rather than other interpretations (e.g., freezing of phosphatidylcholine headgroups) of the exotherm (data not shown).³³ The temperature

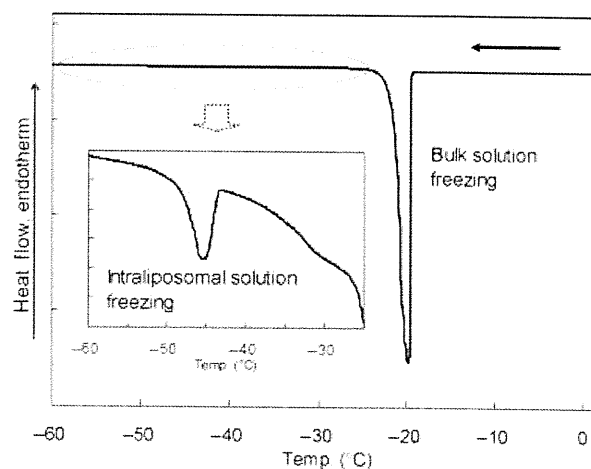


Figure 1. Cooling thermogram of a frozen DPPC liposome suspension. An aliquot (10 μ L) of liposome suspension (4% lipid, w/w) in Tris-HCl buffer (10 mM, pH 7.4) was cooled from room temperature to -70°C at 5°C/min.

of the bulk solution freezing peak varied greatly between the scans. Some suspensions also showed a broad exotherm at approximately -30°C . The exotherm suggested the freezing of solutions released from the liposomes (dehydration) and/or freezing of the internal solutions initiated by external ice crystals that penetrated through the membrane.^{12,16,34} The varied shape and overlapping of the peak with the large bulk solution freezing exotherm made further characterization difficult in this study. The frozen liposome suspensions showed only a gradual shift of the thermogram before the large ice melting endotherm during their heating scans (data not shown). DLS measurement of the DPPC liposome suspensions indicated a mean diameter of 203.9 ± 10.6 nm before the thermal analysis (three different preparations). Standard deviation of the liposome size obtained in each measurement was within 5% of the average value.

The effects of cooling speeds on the internal solution freezing exotherm of liposomes differing in size and lipid composition are shown in Figure 2. Slower

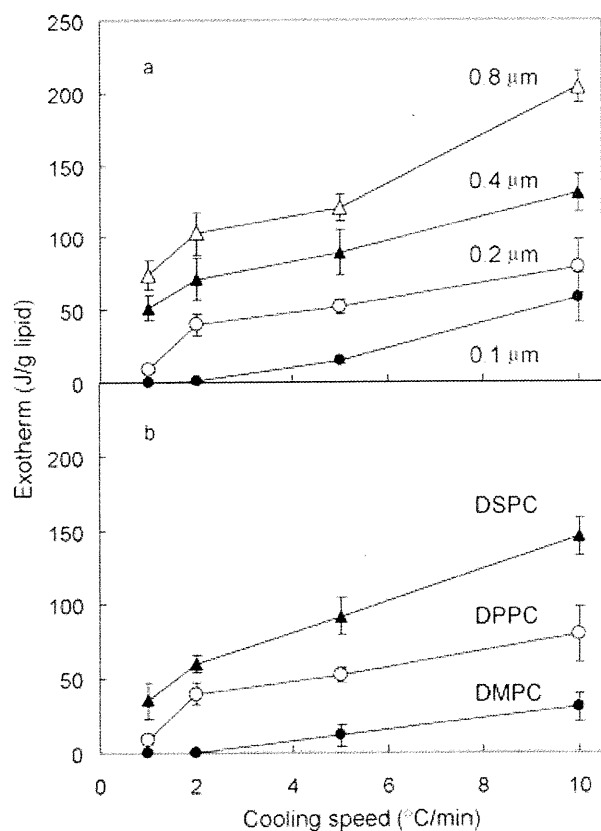


Figure 2. Effects of cooling speed on internal solution freezing exotherm of liposome suspensions with differing (a) extrusion membrane pore sizes (DPPC; 0.1 μm : ●, 0.2 μm : ○, 0.4 μm : ▲, and 0.8 μm : Δ) and (b) lipid compositions (0.2 μm ; DMPC: ●, DPPC: ○, and DSPC: ▲). Aliquots of liposome suspensions (10 μL , 4% lipid in 10 mM Tris-HCl buffer) were cooled at 1–10 $^{\circ}\text{C}/\text{min}$ (average \pm SD, $n = 3$).

cooling of the DPPC liposome suspension (0.2 μm) reduced the exotherm, indicating loss of the supercooled intraliposomal solution during the scan (Fig. 2a; 1 $-2^{\circ}\text{C}/\text{min}$). The extraliposomal ice growth and concomitant concentration of solutes should generate osmotic forces that induce water evacuation from liposomes. Reported freeze-induced morphological rearrangement into multilamellar liposomes may also reduce the intraliposomal solution content.⁴ The width of the bulk solution freezing peak got narrower in the slower cooling, suggesting a certain time required for the ice growth (data not shown). On the contrary, the limited effect of the cooling speed on the peak width of the intraliposomal solution freezing exotherm suggested independent ice formation in the individual liposomes. A certain amount of the intraliposomal solution interacting (hydrating) with the membrane lipid and/or solute molecules should remain unfrozen even below the intraliposomal solution freezing temperature.^{11,11}

Reduction of the intraliposomal solution freezing exotherm was more apparent in the DPPC liposome suspensions temporarily (30 min) kept at temperatures between the bulk and the intraliposomal solution freezing during the cooling scan (Fig. 3). The finding that the intraliposomal solution freezing exotherm of a suspension held at -25°C was smaller than those of suspensions held at -30°C or -35°C suggested faster loss of the supercooled solutions in the temperature range just below the bulk solution freezing. Longer exposure to the temperature range should be one of the reasons for the reduction in the exotherms with the slower cooling. On the contrary, holding the suspension at a temperature above the bulk solution freezing temperature showed no apparent effect on the intraliposomal solution freezing

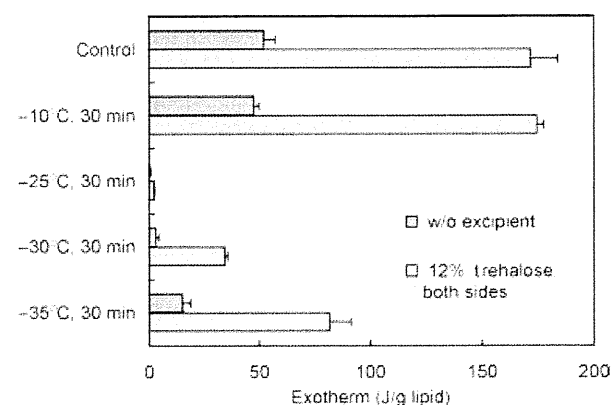


Figure 3. Effect of low temperature holding on internal solution freezing exotherms of DPPC liposome suspensions containing trehalose (0% or 12%, w/w) on both sides of the membrane (10 μL , 4% lipid in Tris-HCl buffer, 0.2 μm). The suspensions were held at different temperatures (-10°C to -35°C) for 30 min during cooling scans at $5^{\circ}\text{C}/\text{min}$.

exotherm. The absence of apparent osmotic driving force may explain the limited effect of storage at above the bulk solution freezing temperature.

The DPPC liposome suspensions extruded through larger pore size filters (e.g., 0.4 and 0.8 μm) showed larger intraliposomal solution freezing exotherms (Fig. 2a). Factors including the possibility of higher initial solution contents per lipid weight, limited membrane disordering associated with the curvature, and slower dehydration due to the increase in multilamellar membranes would explain the large exotherms. Liposomes composed of phosphatidylcholines of different acyl chain lengths showed retention of the intraliposomal solution down to the homogeneous ice formation temperature in the order of DMPC < DPPC < DSPC (Fig. 2b). The intraliposomal solution freezing exotherm was not observed in the thermal analysis of POPC liposome suspensions (data not shown). All the liposome membranes are below their T_m (POPC: -5°C , DMPC: 24°C , DPPC: 41°C , DSPC: 54°C) at the bulk solution freezing temperature.³⁵ Possible differences in the membrane fluidity and rigidity would cause the freeze-induced dehydration to vary.

Effect of Trehalose Distribution on Freezing Profiles of Liposome Suspensions

The effects of intra- and extraliposomal trehalose on the freezing behavior of liposome suspensions were studied. The DPPC liposome suspensions containing trehalose on both sides of the membrane showed larger intraliposomal solution peaks that suggest reduced solution loss upon the bulk solution freezing. For example, cooling of the 0.2 μm DPPC suspensions at $10^\circ\text{C}/\text{min}$ resulted in exotherms of approximately 80 and 200 J/g lipid, respectively, in the absence and presence of trehalose (Figs. 2 and 4). The addition of trehalose also lowered the peak temperature of the exotherm (approx. 3°C at 12% trehalose, w/w).^{18,34} The trehalose-containing liposome lost a larger amount of the internal supercooled solution during the slower cooling of the suspensions. Temporary pausing of the cooling scan suggested a faster loss of the supercooled solution near the bulk solution freezing temperature (-25°C), also in the trehalose-containing liposome suspensions (Fig. 3). The addition of various low-molecular-weight saccharides and polyols to both sides of the lipid membrane increased the freezing exotherm of the intraliposomal solutions, suggesting that slower freeze-induced dehydration occurred due to the colligatively determined osmotic effect (Fig. 5). The limited effect of dextran on the exotherm could be explained by its lower molar concentration and its possible exclusion from the vicinity of the liposomes in the freeze-concentrated non-ice phase.³⁶ The large (0.4 and 0.8 μm) or lower fluidity (DSPC) liposomes retained higher amounts of

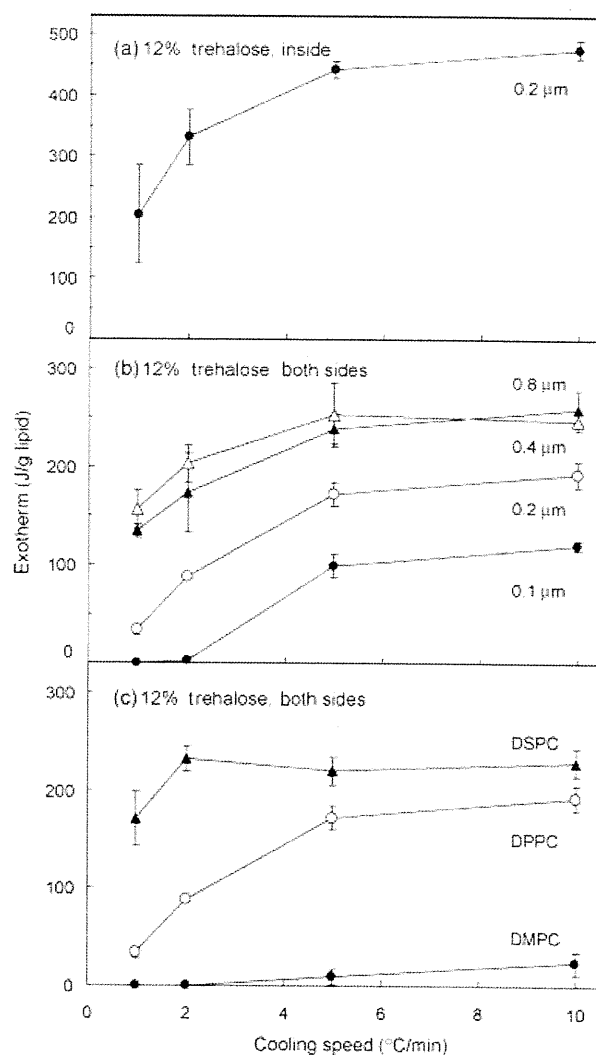


Figure 4. Internal solution freezing exotherms of liposome suspensions containing trehalose (12%, w/w) on (a) the inside and (b, c) both sides of liposomes. Aliquots of suspensions (10 μL , 4% lipid in 10 mM Tris-HCl buffer) containing liposomes with (b) differing extrusion membrane pore sizes (DPPC; 0.1 μm : \bullet , 0.2 μm : \circ , 0.4 μm : \blacktriangle , and 0.8 μm : \triangle) and (c) lipid compositions (0.2 μm ; DMPC: \bullet , DPPC: \circ , and DSPC: \blacktriangle) were cooled at 1 – $10^\circ\text{C}/\text{min}$ (average \pm SD, $n = 3$).

freezable intraliposomal solution in the presence of trehalose on both sides of the membrane (Figs. 4b and 4c).

1,2-Dipalmitoyl-*sn*-glycero-3-phosphocholine liposomes containing trehalose on one side of the membrane showed different freezing behaviors. The addition of higher concentration trehalose to the extraliposomal media reduced the intraliposomal solution freezing exotherm (Fig. 6). The difference in the osmotic pressures across the membrane should induce solution flow that dehydrates the liposomes both prior to cooling and after the bulk solution freezing. The

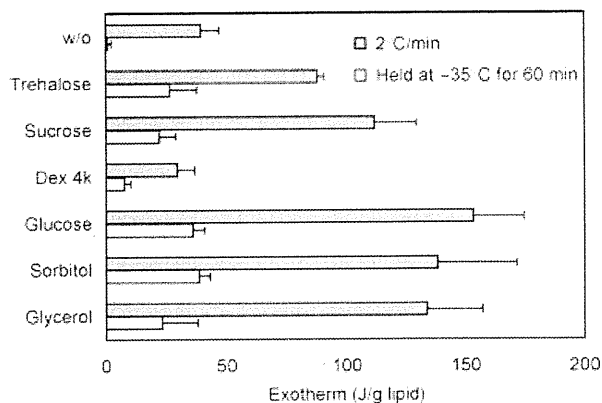


Figure 5. Effect of various extraliposomal solutes (12%, w/w) on internal solution freezing exotherms of DPPC liposome suspensions (10 μ L, 4% lipid in 10 mM Tris-HCl buffer, 0.2 μ m) obtained via cooling scans at 2°C/min (average \pm SD, $n = 3$). Some suspensions were held at -35°C for 60 min during the scan.

absence of a broad exotherm between the bulk and intraliposomal solution freezing peaks suggested that liposome dehydration before the bulk solution freezing (e.g., osmotic shrinkage) had occurred rather than the freeze-induced dehydration (data not shown).

Other low-molecular-weight saccharides and polyols in the extraliposomal media also reduced the intraliposomal solution freezing exotherms of the DPPC liposomes (Fig. 7). The extraliposomal dextran showed smaller effect to reduce the exotherm compared with the lower-molecular-weight excipients. Prior heat treatment of the liposome suspensions at above T_m of DPPC (45°C, 3 min), apparently increased the intraliposomal solution freezing exotherm of the suspensions containing the externally added glycerol or DMSO. Membrane disordering at and above the

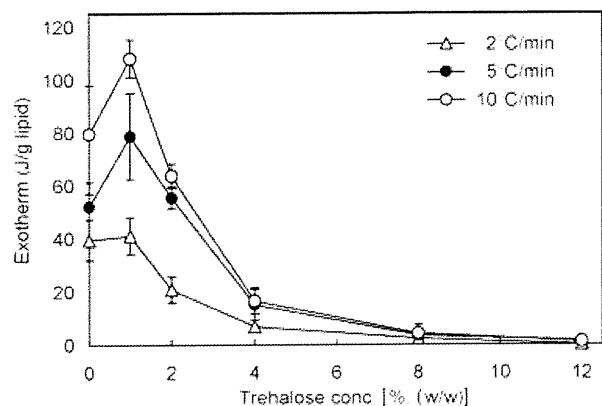


Figure 6. Effect of extraliposomal trehalose (0%–12%, w/w) on internal solution freezing exotherms of DPPC liposome suspensions (10 μ L, 4% lipid in 10 mM Tris-HCl buffer, 0.2 μ m) obtained by cooling at 2°C/min (Δ), 5°C/min (\bullet), or 10°C/min (\circ) (average \pm SD, $n = 3$).

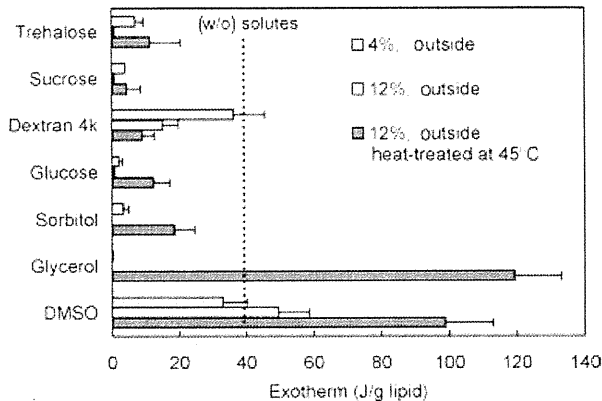


Figure 7. Effect of various extraliposomal solutes (4% and 12%, w/w) on internal solution freezing exotherms of DPPC liposomes obtained via cooling scans of suspensions (10 μ L, 4% DPPC in 10 mM Tris-HCl buffer, 0.2 μ m) from room temperature to -70°C at 2°C/min. Some suspensions were heat-treated at 45°C for 3 min before the cooling analysis (average \pm SD, $n = 3$).

transition temperature should allow an influx of the highly permeable small solute molecules, and should, thus, reduce the osmotic effect that dehydrates the liposomes.

The effect of intraliposomal trehalose on the freezing behavior of DPPC liposomes was also studied (Fig. 4a). The suspensions containing trehalose predominantly inside the liposomes showed apparently larger exotherms than those of other suspensions. The absence of the baseline shift at the trehalose transition temperature of maximally freeze-concentrated solutes (T_g') in the heating scan confirmed the low trehalose concentration outside the liposomes (data not shown). Liposomes prepared by extrusion often contain an amount of internal solution that was insufficient to fill the completely spherical structure, which allows inward water flow across the membrane upon exposure of liposomes to lower osmolarity solutions.³⁷ An increase in the intraliposomal solution content due to osmotic swelling in the initial suspension and limited freeze-induced dehydration can explain the larger ice formation peaks. These results indicated that the osmotic effect made a significant contribution to the freezing behavior of liposomes.

Kinetic stability of the trehalose-containing supercooled intraliposomal solutions was studied to elucidate their relevance in freeze-drying process (Fig. 8). Some liposome suspensions (e.g., trehalose-containing 0.8 μ m DPPC liposome) showed small but apparent intraliposomal solution freezing peaks in the scans after a slower cooling (0.5°C/min) followed by being held at -35°C (180 min). The result suggested that some liposomes retain certain amount of internal solutions during freezing segment of pharmaceutical formulation lyophilization usually

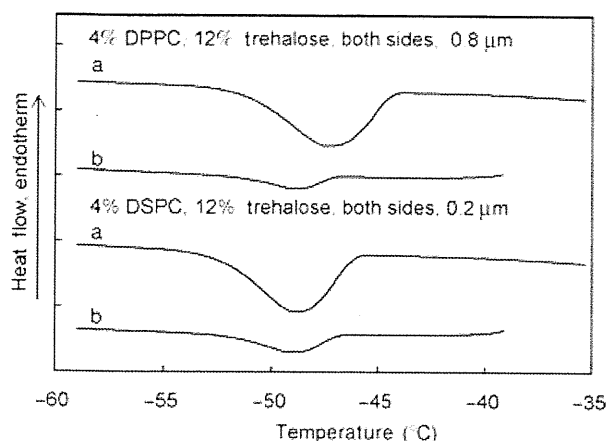


Figure 8. Cooling thermograms of DPPC (0.8 μm) and DSPC (0.2 μm) liposome suspensions containing trehalose (12%, w/w) on both sides of the membrane (10 μL , 4% lipids in 10 mM Tris-HCl buffer). The suspensions were cooled at 5°C/min (a) from room temperature or (b) after slow cooling (0.5°C/min) with a temporary pause at -35°C (180 min).

performed via slow cooling (e.g., 0.2–0.5°C/min) down to -35°C to -50°C on the lyophilizer shelf.^{38,39} The lower product temperature during the process should lead to freezing of the intraliposomal solutions by the homogeneous ice nucleation mechanism.

Effect of Freeze-Thawing on CF-Encapsulated Liposomes

The relationship between trehalose-induced changes in the liposome freezing behavior and functional stability of liposomes upon freeze-thawing was studied (Figs. 9 and 10). The CF-loaded DPPC liposomes were subjected to thermal analysis and freeze-thawing marker-retention study (a) without trehalose, (b) with trehalose on both sides of the membrane, (c) with trehalose in the intraliposomal solution, or (d) with trehalose in the extraliposomal media. A lower concentration (25 mM; approx. 0.94%, w/w) of CF compared with those in other retention studies (e.g., 100 mM) was used for the experiment to reduce its osmotic effect on the freezing behavior of the liposomes. A thermal transition ($T_g' = -36.2^\circ\text{C}$) and absence of other peaks in the heating process of a frozen CF solution (25 mM in Tris-HCl buffer, pH 7.4) indicated that the solute was in a noncrystalline state in the freeze-concentrated phase. The CF-loaded liposome suspensions showed small intraliposomal solution freezing exotherms essentially identical to those of the marker-free samples in the absence of trehalose (Figs. 2 and 9). The liposomes lost a large fraction of the markers upon freeze-thawing of the trehalose-free suspensions cooled down to -35°C (below bulk solution freezing temperature) and -70°C (below intraliposomal solution freezing temperature) at all speeds (Fig. 10).

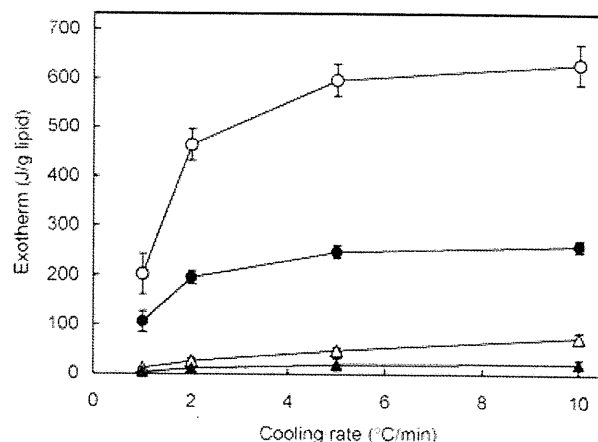


Figure 9. Internal solution freezing exotherms of carboxyfluorescein (25 mM)-containing DPPC liposome suspensions (10 μL , 4% DPPC in 10 mM Tris-HCl buffer, 0.2 μm) without (Δ) or with 12% trehalose on the outside (\blacktriangle , inside (\circ), or both sides (\bullet) of the liposome membrane scanned from room temperature at 1–10°C/min (average \pm SD, $n = 3$).

The DPPC liposomes containing trehalose on both sides of the membrane retained higher intraliposomal solution and encapsulated CF contents under faster cooling (5 and 10°C/min). Small changes of the marker retention in the fast cooling of the suspensions down to -35°C and -70°C suggested that the intraliposomal freezing by itself is not a main cause of the severe marker leakage, at least in the presence of trehalose. A large loss of the intraliposomal solution and

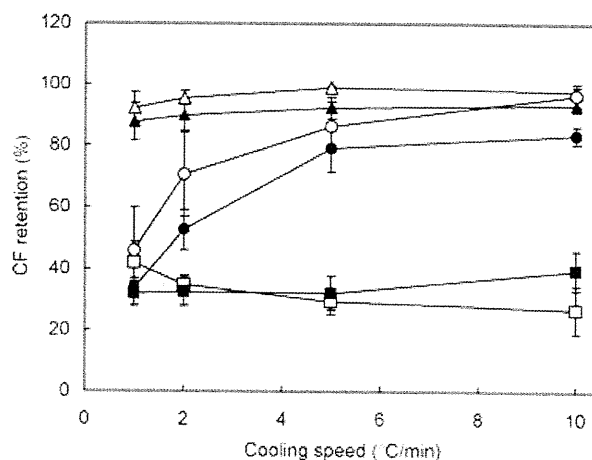


Figure 10. Effect of freeze-thawing on retention of carboxyfluorescein (CF) encapsulated in DPPC liposomes. Aliquots of CF (25 mM)-containing DPPC liposome suspension (10 μL , 4% lipid in 10 mM Tris-HCl buffer, 0.2 μm) without (\square , \blacksquare) or with 12% trehalose on the outside (Δ , \blacktriangle) or both sides (\circ , \bullet) of the liposome membrane were cooled from room temperature to -35°C (open symbols) or -70°C (closed symbols) at 1–10°C/min, and then heated at 10°C/min (average \pm SD, $n = 3$).

an accompanying apparent leakage of the marker in the slowly cooled suspensions suggested that membrane damage had occurred that allowed outbound flow of the marker-containing solution during the freezing process. Experiencing the fast-dehydrating temperature range twice in a freeze–thawing cycle should explain the larger change in marker retention compared with that of the intraliposomal freezing exotherm obtained in some cooling procedures. Suspensions containing CF and trehalose only in the intraliposomal solution also showed large intraliposomal solution freezing exotherms (Figs. 4a and 9). Solidification of the suspensions upon freeze–thawing, which hindered the CF retention measurement, confirmed the requirement of trehalose in the extraliposomal media (data not shown).¹⁶

The externally added trehalose (12%) reduced the CF leakage from the DPPC liposomes upon freeze–thawing at all cooling speeds. The suspensions showed a minor exotherm during the intraliposomal solution freezing. Possible osmotic shrinkage prior to freezing is the likely explanation for the limited internal solution content and the high retention of the encapsulated marker.^{4,22,26} The addition of trehalose to the extraliposomal media (12%) induced leakage of less than 1% of the encapsulated CF at room temperature (data not shown).⁴⁰ Changes in the color of CF-containing liposome suspensions from yellow to orange by the extraliposomal trehalose suggested an increasing intraliposomal marker concentration due to outbound water flow through membrane diffusion (osmotic shrinkage). The lower intraliposomal solution contents should lead to the limited freeze-induced dehydration and membrane damage. The extraliposomal saccharides should also protect liposomes from membrane injury due to the growing ice surface, an

excess concentration of unfavorable solutes (e.g., inorganic salts), and direct contact of concentrated liposome membranes as spacer.^{40,39}

Liposome Stabilization by Control of the Osmotic Flow and Internal Freezing

The results indicated varied effect of trehalose on the freezing behavior and functional stability of liposomes upon freeze–thawing depending on its distribution across the membrane. A schematic flow of the liposome freezing behavior is shown in Figure 11. Understanding the physical changes and the encountering stresses should be relevant for strategic stabilization in freeze–thawing and freeze-drying of liposomes. Liposomes prepared by extrusion often do not contain sufficient solutions to fill the spherical structure.^{37,41} Exposure of the liposomes either increases (e.g., osmotic swelling in hypotonic media) or decreases (e.g., osmotic shrinkage in hypertonic media) the internal solution content via water diffusion through the membranes. The bulk and intraliposomal solutions freeze at different temperatures, as the processes are initiated by the heterogeneous and homogeneous ice nucleation mechanisms, respectively. The freeze-induced osmotic dehydration and the intraliposomal solution freezing initiated by membrane-penetrating ice crystals should reduce intraliposomal solution content that freeze at the homogeneous ice nucleation temperature.^{12,16,34,42} Accordingly, the intraliposomal solution should be in the dehydrated, supercooled, or frozen states in the frozen suspensions depending on the formulation and process factors. The absence of crystallizing solutes (e.g., mannitol) allowed observation of the freeze-induced physical changes through thermal analysis.²⁸

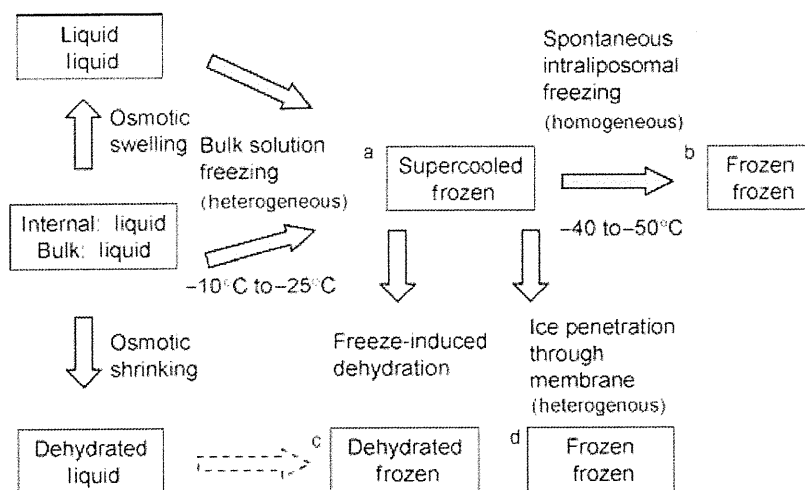


Figure 11. Schematic freezing behaviors of extruded liposome suspensions. The upper and lower rows in each box denote the physical state of the intraliposomal and bulk solutions, respectively. Boxes (a) to (d) indicate suggested physical states of frozen liposome suspensions.

Each step of the freeze-related physical changes induces stresses that affect the stability of liposomes. The growing ice during the bulk and intraliposomal solution freezing should physically damage the liposome membranes. It is possible that the freeze-induced large difference in the osmotic pressure causes larger membrane damage in the DPPC liposomes than in the living cells because of their lower hydraulic permeability, leading to a dehydrating flow of the CF-containing intraliposomal solutions. The liposomes should also experience stresses by ice crystal size growth (Ostwald ripening) and rapid dilution of the surrounding media during the thawing process of the frozen suspensions.^{23,43}

The different stability-determining factors during the freezing process of the marker-loaded liposomes from those of the living cells suggest requirement of different strategies for their stabilization.⁴⁴ Trehalose protected the marker-loaded liposomes through two types of osmotic effects that prevent the freeze-induced internal solution loss during freeze-thawing. The addition of trehalose to both sides of the liposome membrane prevented both the freeze-induced dehydration and water-soluble marker loss, particularly in the higher cooling rate. The marker retention was also achieved by extraliposomal trehalose that osmotically dehydrates the liposomes through outbound water diffusion without apparent CF release in the initial suspensions. The prior dehydration should prevent the freeze-induced membrane damage even in the slower cooling. These osmotic effects should contribute as one of the major mechanisms by which trehalose protects liposomes during the freezing process besides the water-substitution, bulking, and molecular mobility reduction. The liposomes containing sufficiently high concentrations of cryoprotectants can be vitrified without the apparent ice formation by ultrafast cooling (e.g., immersion of small volume suspensions in liquid nitrogen). The vitrification method would not be practical for large-scale freezing of liposome formulations, although it is a popular way to avoid intracellular freezing during cryopreservation of living cells.¹² Formulation and process optimization of liposome pharmaceuticals should be performed through multiple assay methods (e.g., API retention, liposome fusion, aggregation, and activity of encapsulated enzyme) that appropriately detect the changes caused by different stresses.

The varied physical states of the intraliposomal solutions in the frozen suspensions should directly (e.g., membrane damage due to ice growth) or indirectly (e.g., altered excipient-membrane interactions) affect the liposome stability during freeze-drying process and subsequent storage.^{1,5,8,45} The trehalose molecules are required to be distributed in the position spatially accessible to the membrane phospholipids to form the water-substituting interactions that

protect the membrane structure from the dehydration stresses. The higher glass transition temperatures (T_g) of the dried solids and resistance against changes by absorbed water should make trehalose a potent stabilizer for lyophilization and subsequent storage of liposomes and biomacromolecules.³⁹ How the altered freezing behavior affects liposome stability during freeze-drying is an intriguing topic for further study.

The present results indicate the relevance of characterizing the freeze-related physical changes of liposomes for the development of frozen or freeze-dried formulations. The liposome composition and trehalose distribution across the membrane significantly affected the osmotic solution flows that determine the physical states of their intraliposomal solutions and functional stabilities (e.g., CF retention) upon freeze-thawing. Potentially varied molecular interactions between components would also affect liposome stability in the subsequent drying process and in storage. Controlling the osmotically mediated physical changes through formulation design and process optimization would be valuable in the cryopreservation and freeze-drying of liposome pharmaceuticals.

REFERENCES

1. Chen C, Han D, Cai C, Tang X. 2010. An overview of liposome lyophilization and its future potential. *J Control Release* 142:299-311.
2. Misra A, Jinturkar K, Patel D, Lalani J, Chougule M. 2009. Recent advances in liposomal dry powder formulations: Preparation and evaluation. *Expert Opin Drug Deliv* 6:71-89.
3. van Winden EC. 2003. Freeze-drying of liposomes: Theory and practice. *Methods Enzymol* 367:99-110.
4. Wessman P, Edwards K, Mahlin D. 2010. Structural effects caused by spray- and freeze-drying of liposomes and bilayer disks. *J Pharm Sci* 99:2032-2048.
5. Nakagaki M, Nagase H, Ueda H. 1992. Stabilization of the lamellar structure of phosphatidylcholine by complex formation with trehalose. *J Memb Sci* 73:173-180.
6. Crowe JH, Crowe LM, Chapman D. 1984. Preservation of membranes in anhydrobiotic organisms: The role of trehalose. *Science* 223:701-703.
7. Ausborn M, Schreiber H, Brezesinski G, Fabian H, Meyere HW, Nuhna P. 1994. The protective effect of free and membrane-bound cryoprotectants during freezing and freeze-drying of liposomes. *J Control Release* 30:105-116.
8. Crowe JH, Crowe LM, Carpenter JF, Rudolph AS, Wistrom CA, Spargo BJ, Anchordoguy TJ. 1988. Interactions of sugars with membranes. *Biochim Biophys Acta* 947:367-384.
9. Wolfe J, Bryant G. 1999. Freezing, drying, and/or vitrification of membrane-solute-water systems. *Cryobiology* 39:103-129.
10. Lovelock JE. 1954. The protective action of neutral solutes against haemolysis by freezing and thawing. *Biochem J* 56:265-270.
11. Rasmussen DH, Macaulay MN, MacKenzie AP. 1975. Supercooling and nucleation of ice in single cells. *Cryobiology* 12:328-339.
12. Mazur P. 1984. Freezing of living cells: Mechanisms and implications. *Am J Physiol* 247:C125-C142.

13. Shirakashi R, Tanasawa I. 1998. Method of designing pre-freezing protocol in cryopreservation of biological materials. *Ann N Y Acad Sci* 858:175–182.
14. Mathias SF, Franks F, Hatley RH. 1985. Preservation of viable cells in the undercooled state. *Cryobiology* 22:537–546.
15. Siow LF, Rades T, Lim MH. 2007. Characterizing the freezing behavior of liposomes as a tool to understand the cryopreservation procedures. *Cryobiology* 55:210–221.
16. Siow LF, Rades T, Lim MH. 2008. Cryo-responses of two types of large unilamellar vesicles in the presence of non-permeable or permeable cryoprotecting agents. *Cryobiology* 57:276–285.
17. Talsma H, Van Steenberg MJ, Crommelin DJ. 1992. The cryopreservation of liposomes. 2. Effect of particle size on crystallization behavior and marker retention. *Cryobiology* 29:80–86.
18. Charoenrein S, Reid DS. 1989. The use of DSC to study the kinetics of heterogeneous and homogeneous nucleation of ice in aqueous systems. *Thermochim Acta* 156:373–381.
19. Seki S, Kleinmans FW, Mazur P. 2009. Intracellular ice formation in yeast cells vs. cooling rate: Predictions from modeling vs. experimental observations by differential scanning calorimetry. *Cryobiology* 58:157–165.
20. Bronshteyn VL, Steponkus PL. 1993. Calorimetric studies of freeze-induced dehydration of phospholipids. *Biophys J* 65:1853–1865.
21. Lefevre T, Toscani S, Picquart M, Dugue J. 2002. Crystallization of water in multilamellar vesicles. *Eur Biophys J* 31:126–135.
22. Siminovitch D, Chapman D. 1971. Liposome bilayer model systems of freezing living cells. *FEBS Lett* 16:207–212.
23. Talsma H, Steenberg MJV, Crommelin DJA. 1991. The cryopreservation of liposomes: 3. Almost complete retention of a water-soluble marker in small liposomes in a cryoprotectant containing dispersion after a freezing/thawing cycle. *Int J Pharm* 77:119–126.
24. Harrigan PR, Madden TD, Cullis PR. 1990. Protection of liposomes during dehydration or freezing. *Chem Phys Lipids* 52:139–149.
25. Higgins J, Hodges NA, Olliff CJ, Phillips AJ. 1986. Factors influencing cryoprotective activity and drug leakage from liposomes after freezing. *J Pharm Pharmacol* 38:259–263.
26. Hupfeld S, Moen HH, Ausbacher D, Haas H, Brandl M. 2010. Liposome fractionation and size analysis by asymmetrical flow field-flow fractionation/multi-angle light scattering: Influence of ionic strength and osmotic pressure of the carrier liquid. *Chem Phys Lipids* 163:141–147.
27. Ohtake S, Schebor C, Palecek SP, de Pablo JJ. 2005. Phase behavior of freeze-dried phospholipid-cholesterol mixtures stabilized with trehalose. *Biochim Biophys Acta* 1713:57–64.
28. Talsma H, van Steenberg MJ, Salemink PJ, Crommelin DJ. 1991. The cryopreservation of liposomes. 1. A differential scanning calorimetry study of the thermal behavior of a liposome dispersion containing mannitol during freezing/thawing. *Pharm Res* 8:1021–1026.
29. MacDonald RC, MacDonald RI, Menco BP, Takeshita K, Subbarao NK, Hu LR. 1991. Small-volume extrusion apparatus for preparation of large, unilamellar vesicles. *Biochim Biophys Acta* 1061:297–303.
30. Kristiansen J. 1992. Leakage of a trapped fluorescent marker from liposomes: Effects of eutectic crystallization of NaCl and internal freezing. *Cryobiology* 29:575–584.
31. Bartlett GR. 1959. Phosphorus assay in column chromatography. *J Biol Chem* 234:466–468.
32. Kaasgaard T, Mouritsen OG, Jørgensen K. 2003. Freeze/thaw effects on lipid-bilayer vesicles investigated by differential scanning calorimetry. *Biochim Biophys Acta* 1615:77–83.
33. Wu WG, Chi LM, Yang TS, Fang SY. 1991. Freezing of phosphocholine headgroup in fully hydrated sphingomyelin bilayers and its effect on the dynamics of nonfreezable water at subzero temperatures. *J Biol Chem* 266:13602–13606.
34. Rall WF, Mazur P, McGrath JJ. 1983. Depression of the ice-nucleation temperature of rapidly cooled mouse embryos by glycerol and dimethyl sulfoxide. *Biophys J* 41:1–12.
35. Nagle JF, Wilkinson DA. 1978. Lecithin bilayers. Density measurement and molecular interactions. *Biophys J* 23:159–319.
36. Koster KL, Lei YP, Anderson M, Martin S, Bryant G. 2000. Effects of vitrified and nonvitrified sugars on phosphatidylcholine fluid-to-gel phase transitions. *Biophys J* 78:1932–1946.
37. Mui BL, Cullis PR, Evans EA, Madden TD. 1993. Osmotic properties of large unilamellar vesicles prepared by extrusion. *Biophys J* 64:443–453.
38. Akers MJ, Vasudevan V, Stickelmeyer M. 2002. Formulation development of protein dosage forms. *Pharm Biotechnol* 14:47–127.
39. Nail SL, Jiang S, Chongprasert S, Knopp SA. 2002. Fundamentals of freeze-drying. *Pharm Biotechnol* 14:281–360.
40. Blok MC, van Deenen LL, De Gier J. 1976. Effect of the gel to liquid crystalline phase transition on the osmotic behaviour of phosphatidylcholine liposomes. *Biochim Biophys Acta* 433:1–12.
41. Pencer J, White GF, Hallett FR. 2001. Osmotically induced shape changes of large unilamellar vesicles measured by dynamic light scattering. *Biophys J* 81:2716–2728.
42. Suzuki T, Komatsu H, Miyajima K. 1996. Effects of glucose and its oligomers on the stability of freeze-dried liposomes. *Biochim Biophys Acta* 1278:176–182.
43. Grabielle-Madelmont C, Perron R. 1983. Calorimetric studies on phospholipid-water systems: II. Study of water behavior. *J Colloid Interface Sci* 95:483–493.
44. Hubel A, Darr TB, Chang A, Dantzig J. 2007. Cell partitioning during the directional solidification of trehalose solutions. *Cryobiology* 55:182–188.
45. Ohtake S, Schebor C, de Pablo JJ. 2006. Effects of trehalose on the phase behavior of DPPC-cholesterol unilamellar vesicles. *Biochim Biophys Acta* 1758:65–73.

Impact of Heat Treatment on the Physical Properties of Noncrystalline Multisolute Systems Concentrated in Frozen Aqueous Solutions

KEN-ICHI IZUTSU, CHIKAKO YOMOTA, TORU KAWANISHI

National Institute of Health Sciences, Setagaya, Tokyo 158-8501, Japan

Received 8 April 2011; revised 23 June 2011; accepted 24 June 2011

Published online 20 July 2011 in Wiley Online Library (wileyonlinelibrary.com). DOI 10.1002/jps.22706

ABSTRACT: The purpose of this study was to elucidate the effect of heat treatment on the miscibility of multiple concentrated solutes that mimic biopharmaceutical formulations in frozen solutions. The first heating thermal analysis of frozen solutions containing either a low-molecular-weight saccharide (e.g., sucrose, trehalose, and glucose) or a polymer (e.g., polyvinylpyrrolidone and dextran) and their mixtures from -70°C showed a single transition at glass transition temperature of maximally freeze-concentrated solution (T_g') that indicated mixing of the freeze-concentrated multiple solutes. The heat treatment of single-solute and various polymer-rich mixture frozen solutions at temperatures far above their T_g' induced additional ice crystallization that shifted the transitions upward in the following scan. Contrarily, the heat treatment of frozen disaccharide-rich solutions induced two-step heat flow changes (T_g' splitting) that suggested separation of the solutes into multiple concentrated noncrystalline phases, different in the solute compositions. The extent of the T_g' splitting depended on the heat treatment temperature and time. Two-step glass transition was observed in some sucrose and dextran mixture solids, lyophilized after the heat treatment. Increasing mobility of solute molecules during the heat treatment should allow spatial reordering of some concentrated solute mixtures into thermodynamically favorable multiple phases. © 2011 Wiley-Liss, Inc. and the American Pharmacists Association *J Pharm Sci* 100:5244–5253, 2011

Keywords: freezing; freeze-drying; miscibility; phase separation; stabilization; formulation; thermal analysis; calorimetry (DSC); excipients

INTRODUCTION

Freeze-drying is a popular method of formulating certain biopharmaceuticals (e.g., therapeutic proteins and vaccines) and molecular assembly drug delivery systems (e.g., liposomes) that are not sufficiently stable in aqueous solutions during storage and distribution. Formulation and process design that protect the integrity of their higher-order structure from irreversible damages caused by various stresses (e.g., low temperature and dehydration) during the process and storage is particularly important to ensure the quality of the highly potent pharmaceuticals.^{1–5} The growing clinical significance of therapeutic proteins and liposomes makes their miscibility with nonreducing disaccharides (e.g., sucrose and trehalose) in frozen

solutions and subsequently dried solids an intriguing topic because their thermodynamic and kinetic stabilization mechanisms, namely water-substituting direct molecular interactions and mobility-limiting embedment in glass-state solids, both require the mixing of heterogeneous molecules.^{6–10}

Assessing and controlling the component miscibility in noncrystalline solid formulations, however, are often challenging. Thermal analysis and several spectroscopic methods have been applied to estimate the miscibility of ingredients in colyophilized solids and molecular dispersion solid formulations.^{6,8–11} Profiles of glass transition temperatures (T_g s) indicate nonideal mixing of colyophilized disaccharides and polymers (e.g., trehalose and dextran) in some solids.^{9,10} The local inhomogeneity of a disaccharide and a polymer [e.g., polyvinylpyrrolidone (PVP) and lysozyme] in amorphous freeze-dried or hot melt-extruded mixture solids has also been reported in studies using novel spectroscopic techniques [e.g., microscopic

Correspondence to: Ken-ichi Izutsu (Telephone: +81-33700-1141; Fax: +81-33707-6950; E-mail: izutsu@nihs.go.jp)

Journal of Pharmaceutical Sciences, Vol. 100, 5244–5253 (2011)
© 2011 Wiley-Liss, Inc. and the American Pharmacists Association

near-infrared (NIR) and Raman imaging, X-ray powder diffraction (XRPD) coupled with computation of pair distribution functions].^{6,8,11} The broad spectrum, small domains, and difficulties in the handling of the amorphous solids, however, limit the information available using these methods.

Elucidating how each step of the freeze-drying process affects the component miscibility would be another approach to the rational development of stable formulations. The freeze-drying process consists of freezing, primary drying (ice sublimation), and secondary drying (removal of residual water) segments.^{12,13} The freezing of aqueous solutions concentrates the solutes (70%–80%, w/w) into highly viscous supercooled solutions surrounding ice crystals. The increasing concentration separates certain polymer mixtures [e.g., PVP and dextran, polyethylene glycol (PEG) and dextran] or a polymer and an inorganic salt (e.g., PVP and potassium phosphate) that were originally miscible in an aqueous solution into multiple concentrated phases rich in one of the polymers through a thermodynamic mechanism that also induces aqueous two-layer systems.^{14–19} Thermal analysis of frozen solutions provides glass transition temperature of maximally freeze-concentrated solutions (T_g' s) that are valuable to assess miscibility of noncrystalline solutes.^{20,21} Some polymers (e.g., PEG) tend to crystallize in the phase-separated freeze-concentrated solutions.²² Many other solutes in a solution remain miscible in a highly concentrated viscous solution upon freezing.

The purpose of this study was to elucidate the effect of heat treatment (annealing) of frozen solutions on the miscibility of freeze-concentrated disaccharide and polymer mixtures. Subjecting frozen solutions to heat treatment at above their T_g' is a popular method of inducing ice crystal size growth or crystallization of certain solutes in the pharmaceutical lyophilization.^{12,13,23} The increasing ice crystal size by Ostwald ripening and resulting larger pores in the dried layer allow faster water vapor transition from advancing sublimation interfaces during the primary drying. The crystallization of some low-molecular-weight active pharmaceutical ingredients (APIs) and excipients (e.g., antibiotics and bulking agents) in the frozen solutions results in better chemical stability of the dried formulations.²⁴ The faster ice sublimation should also be an apparent advantage for the efficient freeze-drying of biopharmaceutical and drug delivery system (DDS) formulations; however, the application of the heat treatment to the freeze-drying of structurally and compositionally complex systems should require an understanding of the accompanying physicochemical changes caused by the increasing mobility of solute molecules during the heat treatment.²⁵ For example, heat-induced crystallization of a component salt in some buffer systems

(e.g., sodium phosphate) significantly shift pH of the freeze-concentrated solutions and dried solids, and thus alters the stability of colyophilized proteins.^{26,27} Reported phase separation of freeze-dried trehalose and dextran upon exposure to the higher temperature and humidity²⁸ suggested chances for similar component miscibility changes during the heat treatment of frozen solutions.

Frozen aqueous solutions containing nonreducing disaccharides (e.g., sucrose and trehalose) and polymers (PVP and dextran), which are popular as model systems that mimic the freeze-dried protein formulations and amorphous matrix solid dispersion formulations, were used to study the effect of the heat treatment on the solute miscibility in freeze-concentrated solutions and subsequently dried solids.¹¹ The word “heat treatment” rather than “annealing” is mainly used in the following text to simply describe the operation. The heat treatment of frozen aqueous solutions at temperatures just below T_g' , which induces additional ice formation (devitrification), or post-lyophilization annealing were not addressed in this study.^{29,30} Possible mechanisms of the physical changes and their relevance to the formulation qualities are discussed.

MATERIALS AND METHODS

Materials

All chemicals employed in this study were of analytical grade and were obtained from the following commercial sources: D-(+)-glucose, sucrose, D-(+)-trehalose dehydrate, PVP 10,000, PVP 29,000, and PVP 360,000 (Sigma Chemical, St. Louis, Missouri); dextran 40,000 (MP Biomedicals, Solon, Ohio); and maltotriose (Hayashibara Biochemical Laboratories, Okayama, Japan).

Thermal Analysis of Frozen Solutions and Freeze-Dried Solids

Thermal analysis of the frozen solutions and dried solids was performed by using a differential scanning calorimeter (DSC Q-10; TA Instruments, New Castle, Delaware) and Universal Analysis software (TA Instruments). Aliquots of aqueous solutions (10 μ L) in aluminum cells were cooled from room temperature to -70°C at $10^\circ\text{C}/\text{min}$. The first heating scan of the frozen solution at $5^\circ\text{C}/\text{min}$ was posed at varied temperatures (-25°C to -5°C , -5°C unless otherwise mentioned), and then maintained at the temperature for periods of various lengths (1–480 min, 30 min unless otherwise mentioned). After the sample solutions were cooled again to -70°C , the second heating scan was performed at a scanning rate of $5^\circ\text{C}/\text{min}$. Solids (~ 2 mg) lyophilized in aluminum DSC cells were used in the thermal analysis to reduce water vapor

absorption during the sample preparation. The cells were closed hermetically and then subjected to the thermal analysis from -20°C at $5^{\circ}\text{C}/\text{min}$ under a nitrogen gas flow. The glass transition temperatures (T_g' and T_g) were obtained from the maximum inflection point of the discontinuities in the heat flow curves. The two-step heat flow changes observed in the second scan of some heat-treated frozen solutions were provisionally described as lower temperature ($T_{g'2L}$) and higher temperature ($T_{g'2H}$) transitions.

Freeze-Drying

A freeze-drier (FreeZone-6; Labconco, Kansas City, Missouri) was used for lyophilization. Aluminum thermal analysis hermetic pans (TA Instrument) filled with aqueous excipient solutions ($10\ \mu\text{L}$) were placed inside of flat-bottom glass vials (13 mm in diameter; Nichiden-Rika Glass, Kobe, Japan). The vials containing the solution-filled DSC cells or larger volumes of aqueous solutions (1.0 mL, 21 mm diameter vial) transferred to the lyophilizer shelf were cooled to -36°C at $0.5^{\circ}\text{C}/\text{min}$, and then maintained at this temperature for 2 h before the primary drying process. Heat treatment of the frozen solutions was performed at -5°C for 1 h before the second cooling down to -36°C . The frozen solutions were dried under a vacuum (4.0 Pa), whereas the shelf temperature was maintained at -36°C for 24 h, -30°C for 6 h, -24°C for 6 h, and 35°C for 6 h. The shelf was heated at a rate of $0.2^{\circ}\text{C}/\text{min}$ between the thermal steps. The vials were closed with rubber stoppers under a vacuum.

RESULTS AND DISCUSSION

Heat Treatment of Frozen Disaccharide and PVP Mixture Solutions

Frozen aqueous solutions containing varied concentration ratios of sucrose and PVP 29,000 (total 20%, w/w) were subjected to thermal analysis to examine the effect of the heat treatment (Fig. 1). Derivative thermograms of the frozen solutions obtained in the first heating scans (dotted lines) and the second heating scans (solid lines) after heat treatments at -5°C for 30 min showed peaks at T_g' , where the step changes of the heat flow are observed in the original temperature scans. The single-solute frozen 20% sucrose and PVP 29,000 solutions presented T_g' 's at -33.9°C and -23.2°C , respectively, in the first scans. Smaller transitions at lower temperatures (sucrose: -45.6°C , PVP 29,000: -34.4°C) were also observed.^{31,32} The heat treatment induced a small (1°C – 2°C) upward shift of the main T_g' 's in the second heating scan, suggesting that further solute concentration occurred by means of additional ice crystallization in these frozen solutions.²⁹ The T_g' of the

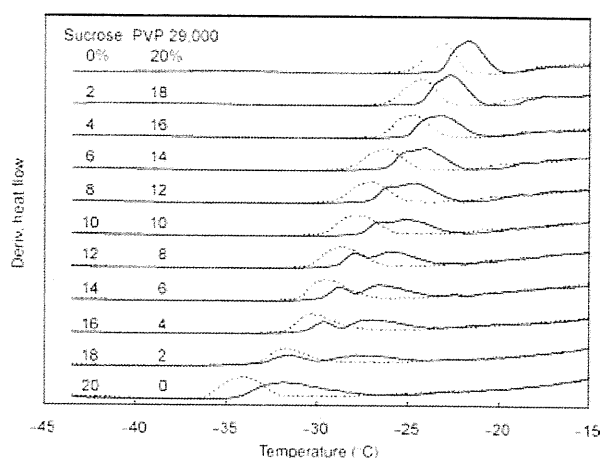


Figure 1. Derivative thermograms of frozen solutions ($10\ \mu\text{L}$) containing sucrose and PVP 29,000 at varied concentration ratios obtained in the first heating scans from -70°C at $5^{\circ}\text{C}/\text{min}$ (dotted lines) and in the second scans after a heat treatment at -5°C for 30 min (solid lines).

frozen sucrose solution became broader upon application of the heat treatment.

The frozen solutions containing both sucrose and PVP 29,000 (total: 20%, w/w) showed single T_g' 's in the first heating scans. The transition temperatures that moved between those of the component solutes suggested mixing of the solutes in the freeze-concentrated nonice phase. The heat treatment at -5°C for 30 min altered the shape and temperature of the T_g' 's differently, depending on the solute compositions. The single T_g' 's of PVP-rich frozen solutions shifted to higher temperatures (1°C – 2°C) upon application of the heat treatment. The same heat treatment induced two-step changes of the heat flow in the frozen solutions containing higher concentration ratios of sucrose (e.g., 10%–18% sucrose): these changes appeared as two peaks in the derivative thermograms. These frozen solutions also showed much smaller thermal transitions at -50°C to -40°C (data not shown). The broad nature of these lower-temperature transitions prevented detailed analysis in this study.

The effect of the heat treatment temperature and time on the thermal properties of the frozen multi-solute solutions was studied to further elucidate the physical changes that occurred. The frozen solutions containing 14% sucrose and 6% PVP 29,000 showed time-dependent splitting of the T_g' peak by the heat treatment at -5°C (Fig. 2). The broad but apparent two peaks observed after the longer heat treatment (10–480 min) strongly suggested the separation into two different transition temperature states rather than toward a particular single- T_g' state. Figure 3 shows the effect of the heat treatment temperatures (-25°C to -5°C) on the T_g' 's of frozen solutions